Stability and Dynamic Analysis of Laminated Composite Plates

Assist. Prof. Dr. Widad I. Majeed
Department of Mechanical Engineering
College of Engineering
Baghdad University
Email:wedad_majeed@yahoo.com

Firas H. Tayeh
Department of Mechanical Engineering
College of Engineering
Baghdad University
Email:firas_frs_drsf@yahoo.com

ABSTRACT

Buckling and free vibration analysis of laminated rectangular plates with uniform and non uniform distributed in-plane compressive loadings along two opposite edges is performed using the Ritz method. Classical laminated plate theory is adopted. The static component of the applied in-plane loading are assumed to vary according to uniform, parabolic or linear distributions. Initially, the plate membrane problem is solved using the Ritz method; subsequently, using Hamilton's variational principle, linear homogeneous algebraic equations in terms of unknown are generated, the set of linear algebraic equations can be solved as an Eigen-value problem. Buckling loads for laminated plates with different combinations of boundary conditions are obtained and their effect on the natural frequencies of plate are also investigated. The proposed method is verified by comparing results to data obtained by the finite element method (FEM) using ANSYS program, from experimental program and that obtained by other researchers. Analytical results are also presented to bring out the effects of aspect ratio, boundary conditions, lamination angle, and loading type on the critical buckling load and natural frequency.

Key words: Vibration, stability, anisotropic plates, classical laminated plate theory, Ritz method

تحليل الإستقرارية و الديناميكة لصفائح مركبة طبقية

أ.م.د. وداد ابراهيم مجيد
قسم هندسة الميكانيك
كلية الهندسة / جامعة بغداد

فراس حميزة تايه
قسم هندسة الميكانيك
كلية الهندسة -جامعة بغداد

الخلاصة

أجري في هذا البحث تحليل الانبعاج و الاهتزاز الحر لصفائح طبقية مستطيلة معرضة لأحمال ضاغطة موزعة بشكل منتظم أو غير منتظم على حافتين متعاكستين باستخدام طريقة Ritz. النظرية الكلاسيكية للصفائح الطبقية قد اختيرت لإجراء هذه الدراسة. أختير المكون الساكن للأحمال المسلطة ضمن المستوي ليكون موزع بثلاثة أشكال: منتظم, خطي, و منحني على شكل قطع مكافئ. بدايةً, تم استخدام طريقة Ritz لحل مسألة الصفيحة و الحصول على معادلات خطية جبرية متجانسة كدوال لمجاهيل باستخدام المبدأ التغييري لـ Hamilton ; يتم حل هذه المعادلات كمسألة Eigen-value. تم إيجاد حمل الانبعاج للصفائح الطبقية و التي تكون مثبتة بحدود مختلفة و دراسة تأثير هذه الاحمال على التردد الطبيعي. تم التحقق من النتائج بمقارنتها بنتائج عددية مستحصلة باستخدام برنامج ANSYS و بنتائج مختبرية تجريبية, و كذلك مقارنتها ببعض النتائج المقدمة بواسطة باحثين آخرين. النتائج التحليلية قدمت لدراسة تأثير نسبة الطول الى العرض, حدود التثبيت, زاوية التصفيح, و نوع التحميل على حمل الانبعاج الحرج و التردد الطبيعي.

الكلمات الرئيسية: اهتزاز, استقرارية, صفيحة متباينة الخواص, النظرية الكلاسيكية للصفائح الطبقية, طريقة Ritz.

1. INTRODUCTION

Thin plates of various shapes used in naval and aeronautical structures are often subjected to normal compressive and shearing loads acting in the middle plane of the plate (in-plane loads). Under certain conditions such loads can result in a plate buckling. In many cases, a failure of thin plate elements may be attributed to an elastic instability and not to the lack of their strength. Therefore, plate buckling analysis presents an integral part of the general analysis of a structure, **Ventsel and Krauthammer, 2001**. It is important to note that a plate leading from the stable to unstable configuration of equilibrium always passes through the neutral state of equilibrium, which thus can be considered as a bordering state between the stable and unstable configurations. In the mathematical formulation of elastic stability problems, neutral equilibrium is associated with the existence of bifurcation of the deformations. According to this formulation, the critical load is the smallest load at which both the flat equilibrium configuration of the plate and slightly deflected configuration are possible , **Ventsel and Krauthammer, 2001**. The composite structures whether used in civil, marine or aerospace are subjected to dynamic loads during their operation. Therefore, there exists a need for assessing the natural frequency. Therefore, for assessing the natural frequency of the laminated composite plate structures, the accurate mathematical model is required, **Reddy, et al., 2013**. There are many applications on buckling and stability of composite materials structures in the present industry such as ship hull, crown of the hat-stiffened panel, blended wing body (BWB) Aircraft. Many researchers have studied the stability of composite plates subjected to buckling loads, each one with his own perspective. **Matsunaga, 2000,** analyzed natural frequencies and buckling stresses of cross-ply laminated composite plates by taking into account the effects of shear deformation, thickness change and rotatory inertia. **Leissa and Kang, 2002,** investigated exact solutions for the free vibration and buckling of rectangular plates having two opposite edges simply supported and the other two were clamped, with the simply supported edges subjected to a linearly varying normal stress. **Craciun and Simionescu–Panait, 2004,** considered the internal and superficial instability of a prestressed fiber reinforced orthotropic elastic composite. **Jana and Bhaskar (2007)** examined the effect of a non-uniform distribution of the applied edge loads on their net critical value with in-plane lateral restraint. **Amabili, et al., 2010,** presented an investigation to laminate composite rectangular plates with different boundary conditions subjected to an external point force. **Tang and Wang**, **2011**, investigated the buckling analysis of symmetrically laminated rectangular plates with parabolic distributed in-plane compressive loadings along two opposite edges using the Rayleigh–Ritz method. In the present work, the stability and buckling analysis of laminated composite plate under uniaxial uniform and non-uniform distributed load is performed. Classical laminated plate theory is adopted. Buckling loads for laminated plates with different combinations of boundary conditions are obtained and their effect on the natural frequencies of plate are also investigated.

2. THEORY

This study is based on classical laminated plate theory (CLPT) and used Hamiltons principles to derive the equation of motion. Ritz method is used to solve the principle of minimum potential energy as an Eigen-value problem to get the critical buckling load and natural frequency for different considerations (boundary conditions, aspect ratios, mechanical properties, lamination systems).

2.1 Classical Laminated Plate Theory

The simplest laminated plate theory is the classical laminated plate theory (or CLPT), which is an extension of the Kirchhoff (classical) plate theory to laminated composite plates. It is based on the displacement field, **Reddy, 2004**.

$$u(x,y,z,t) = u_o(x,y,t) - z\frac{\partial w_o}{\partial x}$$

$$v(x,y,z,t) = v_o(x,y,t) - z\frac{\partial w_o}{\partial y}$$

$$w(x,y,z,t) = w_o(x,y,t) \quad (1)$$

where (u_o, v_o, w_o) are the displacement components along the (x, y, z) coordinate directions, respectively, of a point on the midplane (i.e., z = 0). The displacement field implies that straight lines normal to the xy-plane before deformation remain straight and normal to the midsurface after deformation. The Kirchhoff assumption neglects both transverse shear and transverse normal effects; i.e., deformation is due entirely to bending and in-plane stretching.

2.2 Total Mechanical Energy

The first law of thermodynamics or the principle of conservation of energy serves as the foundation for energy-based methods employed in the analysis of structures, including plates. The total mechanical energy (defined as the sum of its potential and kinetic energies) of a particle being acted on by only conservative forces is constant, **Brown, 2007**.

$$E = E_c + \Pi = Constant \quad (2)$$

where E is the total mechanical energy; E_c is the total kinetic energy; Π is total potential energy. The kinetic energy E_c is written as the following form taking in account the transverse deformation only on the vibration frequencies, **Berthelot, 2010**:

$$E_c = \frac{1}{2}\omega^2 \iint I_o w_o^2 dx\, dy \quad (3)$$

where ω is the natural frequency of the plate vibrations and I_o is the moment of inertia of the laminate at point (x, y) given below:

$$I_o = \int_{-h/2}^{h/2} \rho dz = \sum_{k=1}^{L} \rho_k (z_k - z_{k-1}) \quad (4)$$

Where L is the total number of layers in the laminate; k denotes the layer number; h is the thickness of the laminate; z_k and z_{k-1} are distances from the reference plane of the laminate to the two surfaces

of the *kth* ply **Fig. 1** .The total potential energy, Π, consists of the strain energy of internal forces, *U*, and the work of external forces, Ω, i.e. **Reddy, 2004**,

$$\Pi = U + \Omega \tag{5}$$

The strain energy for an anisotropic material is written as, **Kollar, and Springer, 2003**:

$$U = \frac{1}{2}\int_0^b \int_0^a \begin{Bmatrix} k_x \\ k_y \\ k_{xy} \end{Bmatrix}^T \begin{bmatrix} B_{11} & B_{12} & B_{16} & D_{11} & D_{12} & D_{16} \\ B_{21} & B_{22} & B_{26} & D_{21} & D_{22} & D_{26} \\ B_{61} & B_{62} & B_{66} & D_{61} & D_{62} & D_{66} \end{bmatrix} \begin{Bmatrix} k_x \\ k_y \\ k_{xy} \end{Bmatrix} dx\, dy \tag{6}$$

where κ_x, κ_y, and κ_{xy} are the curvatures of the reference plane of the plate defined as:

$$k_x = -\frac{\partial^2 w_o}{\partial x^2}\,, \qquad k_y = -\frac{\partial^2 w_o}{\partial y^2}\,, \qquad k_{xy} = -\frac{2\partial^2 w_o}{\partial x \partial y} \tag{7}$$

[B] and [D] are the coupling and bending stiffness matrices, respectively. The elements of these matrices are (i, j = 1, 2, 6) given as functions of the transformed reduced stiffness matrix elements $\bar{Q}_{ij}$

$$B_{ij} = \frac{1}{2}\sum_{k-1}^{L}\left(\bar{Q}_{ij}\right)_k (z_k^2 - z_{k-1}^2)\ , D_{ij} = \frac{1}{3}\sum_{k-1}^{L}\left(\bar{Q}_{ij}\right)_k (z_k^3 - z_{k-1}^3) \tag{8}$$

By using the relationships between the curvatures and the deflections, the expression of the strain energy for a symmetric layup is as follows:

$$U = \frac{1}{2}\int_0^b \int_0^a \left[D_{11}\left(\frac{\partial^2 w_o}{\partial x^2}\right)^2 + D_{22}\left(\frac{\partial^2 w_o}{\partial y^2}\right)^2 + D_{66}\left(\frac{2\partial^2 w_o}{\partial x \partial y}\right)^2 + 2\left(D_{12}\frac{\partial^2 w_o}{\partial x^2}\frac{\partial^2 w_o}{\partial y^2} + D_{16}\frac{\partial^2 w_o}{\partial x^2}\frac{2\partial^2 w_o}{\partial x \partial y} + D_{26}\frac{\partial^2 w_o}{\partial y^2}\frac{2\partial^2 w_o}{\partial x \partial y}\right)\right] dx\, dy \tag{9}$$

The potential energy is related only to the in-plane distributed loads N_x applied uniaxially to the edges *x=0, a*, and is written as

$$\Omega = -\frac{1}{2}\iint \left[N_x \left(\frac{\partial w_o}{\partial x}\right)^2 \right] dx\, dy \tag{10}$$

N_x is assumed to be distributed load (uniform and not uniform) taking the forms as derived **Fig. 2**:

$$N_x = -N_o\ , N_x = -\frac{4N_o y}{b}\left(1 - \frac{y}{b}\right)\ , N_x = -N_o\left(1 - \frac{y}{b}\right) \tag{11}$$

where N_o is the maximum intensity of the compressive force at the edges $x=0$ and $x=a$.

2.3 Boundary Conditions

The approximate solution is sought in the usual form of a double series in separate variables **Berthelot, 2010**:

$$w_o(x,y) = \sum_{m=1}^{M}\sum_{n=1}^{N} A_{mn} X_m(x) Y_n(y) \tag{12}$$

where M and N are the numbers of half-waves used in the x and y directions, respectively, of a mode shape. The functions $X_m(x)$ and $Y_n(y)$ must constitute functional bases and are chosen so as to satisfy the boundary conditions along the edges $x = 0$, $x = a$, $y = 0$, and y = b. The coefficients A_{mn} are determined by the stationarity conditions:

$$\frac{\partial U}{\partial A_{mn}} = 0 \tag{13}$$

where $m = 1, 2, \ldots, M$ and $n = 1, 2, \ldots, N$. To select an expression for the deflection w_o, the functions $X_m(x)$ and $Y_n(y)$ are selected to satisfy the geometrical boundary conditions for the studied cases:

a- For the case of a simply supported (**SSSS**) plate, the boundary conditions functions along the edges are as follows, **Reddy, 2004**:

$$X_m(x) = sin\frac{m\pi x}{a}\,, \qquad Y_n(y) = sin\frac{n\pi y}{b} \tag{14}$$

b- For the case of a built in (**CCCC**) plate, the functions of the transverse deflection w_o can be taken as follows **Berthelot, 2010**:

$$X_m(x) = cos\,\lambda_m\frac{x}{a} - cosh\,\lambda_m\frac{x}{a} - \gamma_m\left(sin\lambda_m\frac{x}{a} - sinh\lambda_m\frac{x}{a}\right)$$
$$Y_n(y) = cos\,\lambda_n\frac{y}{b} - cosh\,\lambda_n\frac{y}{b} - \gamma_n\left(sin\lambda_n\frac{y}{b} - sinh\lambda_n\frac{y}{b}\right) \tag{15}$$

where $\lambda_m, \lambda_n, \gamma_m,$ and γ_n are constants given in **Table (1)**.

c- In the case where two opposite edges are clamped along $x=0$ and $x=a$ and the other two edges are simply supported along $y=0$ and $y=b$, that can be sampled as (**CSCS**), the transverse deflection w_o functions are as follows **Berthelot, 2010**:

$$X_m(x) = cos\,\lambda_m\frac{x}{a} - cosh\,\lambda_m\frac{x}{a} - \gamma_m\left(sin\lambda_m\frac{x}{a} - sinh\lambda_m\frac{x}{a}\right), \qquad Y_n(y) = sin\frac{n\pi y}{b} \tag{16}$$

d- For the case where the edges along *x=0* and *x=a* are simply supported and the edges along *y=0* and *y=b* are free that can be sampled as (**SFSF**), the functions that satisfy these boundary conditions can be taken as follows **Berthelot, 2010**:

$$X_m(x) = sin\frac{m\pi x}{a}, Y_1(y) = 1\,, Y_2(y) = \sqrt{3}\left(1 - 2\frac{y}{b}\right),$$
$$Y_n(y) = cos\,\lambda_n\frac{y}{b} + cosh\,\lambda_n\frac{y}{b} + \gamma_n\left(sin\lambda_n\frac{y}{b} + sinh\lambda_n\frac{y}{b}\right) \quad (17)$$

The values of λ_n and γ_n are reported in **Table (1)**.

e- When the plate is taken clamped along two opposite edges where *x=0* and *x=a* and free along the others where *y=0* and *y=b* that can be sampled as (**CFCF**), and the functions will be combined as shown below **Berthelot, 2010**:

$$X_m(x) = cos\,\lambda_m\frac{x}{a} - cosh\,\lambda_m\frac{x}{a} - \gamma_m\left(sin\lambda_m\frac{x}{a} - sinh\lambda_m\frac{x}{a}\right),$$
$$Y_1(y) = 1\,, Y_2(y) = \sqrt{3}\left(1 - 2\frac{y}{b}\right)\,, Y_n(y) = cos\,\lambda_n\frac{y}{b} + cosh\,\lambda_n\frac{y}{b} + \gamma_n\left(sin\lambda_n\frac{y}{b} + sinh\lambda_n\frac{y}{b}\right) \quad (18)$$

where $\lambda_m, \lambda_n, \gamma_m,$ and γ_n are constants given in **Table (1)**.

2.4 Weak Forms

The Ritz method can be used to determine an approximate solution to the bending, buckling, and natural vibrations of symmetric laminates. The weak form or the statement of the principle of minimum total potential energy for buckling and natural vibration problems is given below, **Reddy, 2004**:

$$0 = \int_0^b \int_0^a \left\{ D_{11}\frac{\partial^2 w_o}{\partial x^2}\frac{\partial^2 \delta w_o}{\partial x^2} + D_{12}\left(\frac{\partial^2 w_o}{\partial y^2}\frac{\partial^2 \delta w_o}{\partial x^2} + \frac{\partial^2 w_o}{\partial x^2}\frac{\partial^2 \delta w_o}{\partial y^2}\right) + D_{22}\frac{\partial^2 w_o}{\partial y^2}\frac{\partial^2 \delta w_o}{\partial y^2} \right.$$
$$+4D_{66}\frac{\partial^2 w_o}{\partial x\partial y}\frac{\partial^2 \delta w_o}{\partial x\partial y} + 2D_{16}\left(\frac{\partial^2 w_o}{\partial x\partial y}\frac{\partial^2 \delta w_o}{\partial x^2} + \frac{\partial^2 w_o}{\partial x^2}\frac{\partial^2 \delta w_o}{\partial x\partial y}\right) + 2D_{26}\left(\frac{\partial^2 w_o}{\partial x\partial y}\frac{\partial^2 \delta w_o}{\partial y^2}\right.$$
$$\left. \left. + \frac{\partial^2 w_o}{\partial y^2}\frac{\partial^2 \delta w_o}{\partial x\partial y}\right) + N_x\frac{\partial w_o}{\partial x}\frac{\partial \delta w_o}{\partial x} - \omega^2(I_o w_o \delta w_o)\right\} dx\,dy \quad (19)$$

where ω denotes the frequency of natural vibration. For buckling analysis, all terms involving frequency of vibration are set to zero, while N_x is eliminated for natural vibration.

2.4.1 Buckling of a simply supported plate

Consider a simply supported rectangular plate made of an orthotropic laminate, the material directions of which coincide with the plate directions. This plate is subjected to uniaxial uniform in-plane compressive forces N_x along the edges $x = 0$ and $x = a$. The total potential energy can be written in the following expression:

$$\Pi = \frac{1}{2}\int_0^b \int_0^a \left[D_{11}\left(\frac{\partial^2 w_o}{\partial x^2}\right)^2 + D_{22}\left(\frac{\partial^2 w_o}{\partial y^2}\right)^2 + 4D_{66}\left(\frac{\partial^2 w_o}{\partial x \partial y}\right)^2 + 2\left(D_{12}\frac{\partial^2 w_o}{\partial x^2}\frac{\partial^2 w_o}{\partial y^2} + D_{16}\frac{\partial^2 w_o}{\partial x^2}\frac{2\partial^2 w_o}{\partial x \partial y} + D_{26}\frac{\partial^2 w_o}{\partial y^2}\frac{2\partial^2 w_o}{\partial x \partial y}\right) + N_x\left(\frac{\partial w_o}{\partial x}\right)^2 \right] dx\, dy \quad (20)$$

The transverse displacement (w_o) is written as mentioned in section 2.3 in the following form:

$$w_o = A_{mn} sin\frac{m\pi x}{a} sin\frac{n\pi y}{b}, \;\; m = 1, 2, \dots, M \text{ and } n = 1, 2, \dots, N \quad (21)$$

Assume a plate of a symmetric layup subjected to uniaxial compression; for a simple case, consider m=n=1:

$$w_o = A_{11} sin\frac{\pi x}{a} sin\frac{\pi y}{b} \quad (22)$$

substituting w_o Eq. (22) in Eq. (20) and performing the differentiation and integration processes, and then by using Eq. (19) , the following representation of the critical buckling load N_{cr} can be obtained:

$$N_{cr} = (9.869D_{11}b^4 + 9.869D_{22}a^4 + 19.739D_{12}a^2b^2 + 39.478D_{66}a^2b^2)/a^2b^4 \quad (23)$$

when *m* and *n* are more than 1, the critical load N_{cr} is determined by solving Eigen value problem. For different arbitrary boundary conditions and *m & n* are greater than 1, the solution becomes more difficult and needs computer programming to determine the critical buckling load.

2.4.2 Vibration of simply supported plate

For vibration problem, the total mechanical energy is written as:

$$E = \frac{1}{2}\int_0^b \int_0^a \left[D_{11}\left(\frac{\partial^2 w_o}{\partial x^2}\right)^2 + 2D_{12}\frac{\partial^2 w_o}{\partial x^2}\frac{\partial^2 w_o}{\partial y^2} + D_{22}\left(\frac{\partial^2 w_o}{\partial y^2}\right)^2 + 4D_{66}\left(\frac{\partial^2 w_o}{\partial x \partial y}\right)^2 + 2\left(D_{12}\frac{\partial^2 w_o}{\partial x^2}\frac{\partial^2 w_o}{\partial y^2} + D_{16}\frac{\partial^2 w_o}{\partial x^2}\frac{2\partial^2 w_o}{\partial x \partial y} + D_{26}\frac{\partial^2 w_o}{\partial y^2}\frac{2\partial^2 w_o}{\partial x \partial y}\right) - I_o\omega^2 w_o^2 \right] dx\, dy \quad (24)$$

The natural frequancy ω is obtained using the same procedure to be as below:

$$\omega = \pm\frac{9.869}{a^2b^2}\,(D_{22}a^4 + D_{11}b^4 + 2D_{12}a^2b^2 + 4D_{66}a^2b^2)^{0.5}/I_o \quad (25)$$

In case of finding the natural frequency under the action of critical buckling force N_{cr}, the total mechanical energy is written as:

$$E=\frac{1}{2}\int_0^b\int_0^a\left[D_{11}\left(\frac{\partial^2 w_o}{\partial x^2}\right)^2+2D_{12}\frac{\partial^2 w_o}{\partial x^2}\frac{\partial^2 w_o}{\partial y^2}+D_{22}\left(\frac{\partial^2 w_o}{\partial y^2}\right)^2+4D_{66}\left(\frac{\partial^2 w_o}{\partial x\partial y}\right)^2+2\left(D_{12}\frac{\partial^2 w_o}{\partial x^2}\frac{\partial^2 w_o}{\partial y^2}\right.\right.$$
$$\left.\left.+D_{16}\frac{\partial^2 w_o}{\partial x^2}\frac{2\partial^2 w_o}{\partial x\partial y}+D_{26}\frac{\partial^2 w_o}{\partial y^2}\frac{2\partial^2 w_o}{\partial x\partial y}\right)+N_{cr}\left(\frac{\partial w_o}{\partial x}\right)^2-I_o\omega^2 w_o^2\right]dx\,dy \qquad (26)$$

The natural frequency under that critical buckling load is found to be:

$$\omega=\pm\frac{1.637}{a^2b^2\sqrt{I_o}}(36.322D_{11}b^4+36.322D_{22}a^4+72.644D_{12}a^2b^2+145.289D_{66}a^2b^2$$
$$+3.680N_{cr}a^2b^4)^{0.5} \qquad (27)$$

The natural frequency given in Eq. (25) and Eq. (27) is the fundamental natural frequency where it occurs at *m=n=1* **Reddy, 2004**.

3. EXPERIMENTAL WORK

The experimental work is performed on a plate composed of Polyester as a matrix reinforced with E-Glass fibers.

3.1 Mold Preparation and Mechanical Properties

Two flat wood panels are shaped as square panels of 35 cm*35 cm, with proper thickness to carry moderate loads; they are used as base and cover of the mold to prepare the desired models. One of the panels is used as the base where the materials are molded up, and the other one is the cover that transferes the pressure from up surface to the surface of the desired plate molded on the base. After weaving a layer of E-glass fibers, the catalyzed resin mixture with hardener must be applied to the fibers carefully to prevent distortion in them during the brushing process until the fibers saturate with the risen. Brushes and rollers are used to diffuse the mix over the fibers, and blades are used to take the air bubbles out of the laminate layers **Fig. 3**. Then the mold is left for a day in room temperature for curing after that we cut the model to the desired dimensions by a proper diamond impregnated wheel, cooled by running water. Before starting the experimental work, the fiber, matrix, and then composite densities are measured see **Table (2)**. Then, the fiber volume fraction is measured experimentally to be 0.323. Tensile test is performed to find the composite mechanical properties. D3039 ASTM is used to formulate the tested specimens. The tensile test led to the mechanical properties of E-Glass/Polyester laminated composite plate listed in **Table (2)**.

3.2 Buckling Test

For buckling test, tow models of E-Glass/Polyester laminated plates are prepared. One of the models is (20 cm*20 cm*0.25 cm, $[0/90]_s$) where the aspect ratio (a/b) is equal to 1, and the other one is (40 cm*20 cm*0.2 cm, $[0/90]_2$) where $a/b = 2$. The models are placed vertically between the testing device jaws, where the machine is of 100 KN capacity. The boundary conditions of the tested plates are simply supported along the top and bottom edges while the left and right edges are left free. The compression is exerted on the upper edge by moving stiff head with a speed of 2 mm/min while the lower head is fixed. For determination of the buckling load, load-displacement

method is used **Fig. 4**. Analytical and Numerical results are determined for the tested models and are presented to verify the found experimental results which are listed in **Table (3)**.

3.3 Experimental Modal Analysis

For free vibration test, a model specimen is manufactured with dimensions of (30 cm*30 cm*0.37 cm) and lamination of $(0/90)_2$. The plate is placed in a structure **Fig. 5.a**, where the boundary conditions are simply supported along the four edges and the real tested area is (25 cm* 25 cm) where the edges of the structure are designed to prevent the plate from moving in z-direction. Calibration operation is performed before the test to ensure that the result from the test is right with less error. The plate is placed in the structure that is already manufactured for this purpose where the boundary conditions are kept to be simply supported. The oscilloscope is viewing the response of the specimen that is loaded with hit by an impact hammer which is connected to the oscilloscope and generates the input load to the specimen. The accelerometer is connected to the charge amplifier which will reduce the frequency noise by filters were built to limit the frequency range to the range of interest. The signal goes from the amplifier to the oscilloscope to analyze it and then present it as wave with tops that will give the frequency of the modes. The hit exerted by the impact hammer on the plate. The FFT solution generated **Fig. 5.b** captured from the oscilloscope monitor in purple color wave. The natural frequency ω_o of the first mode taken from the wave is found to be 0.0331 rad/sec. The non-dimensional natural frequency is calculated as below:

$$\bar{\omega} = \frac{\omega_o a^2}{h}\sqrt{\frac{\rho_c}{E_2}} = \frac{0.0331 * 0.25^2}{0.0037}\sqrt{\frac{1369}{5.881}} = 8.529 \quad (28)$$

The analytical result is found to be $\bar{\omega} = 7.832$ so that the error is 8.9%, and that is an accepted error if some conditions are taken in account such as movement of the structure, accuracy of the devices, and the molding process, etc.. **Fig. 5.b** shows the response wave of the plate in yellow color.

4. RESULTS AND DISCUSSION

This study investigates mainly the effect of the critical buckling load that a composite materials plate can hold on its natural frequency. The results are determined analytically and numerically, and study the effect of boundary conditions, aspect ratio, lamination angle, and type of applied edge load.

4.1 Investigation of Critical Buckling Load

The critical buckling load is studied under some considerations. The load is obtained as the non-dimensional load ($\bar{N}$).

a- Effect of Boundary Conditions

Assume a square symmetric cross-ply [0 90 0] laminate (E_1/E_2 =10, G_{12}=0.6E_2, υ_{12}=0.25) is subjected to uniaxial edge loads. **Table (4)** shows the Nondimensionalized buckling load ($\bar{N} = \frac{N_{cr}b^2}{E_2 h^3}$) that the plate can hold. It shows that the clamped plate along two or four edges can hold buckling load more than plate with simply supported boundary

conditions, especially for the case where the plate is SFSF. In the case where the plate is simply supported or mixed with free edges, it is weak to hold large loads compared with clamped plates. From **Table (4)**, it is observed that the critical buckling load for SFSF decreases by 80.28% compared with CCCC for uniformly loaded plate, 74.6% for parabolic load, and 86.28% for linear load.

b- Effect of aspect ratio

Assume a plate (E_1/E_2 =10, G_{12}=0.6E_2, υ_{12}=0.25) with various aspect ratios. From **Fig. 6.a**, it is observed that the Nondimensionalized buckling load ($\bar{N} = \frac{N_o b^2}{\pi^2 D_{22}}$) for clamped plated decreases rapidly with the increase of the aspect ratio until the aspect ratio is 1.6 where $\bar{N}$ starts to increase again for the three types of loading; but for SFSF which is the weaker case, the plate buckles with close values of loads for larger aspect ratios than 1.6 with no increasing in buckling load. Hence, the increasing of aspect ratio decreases buckling load as verified with **Reddy, 2004, Hu, and Abatan, 2003**. **Fig. 6.b** shows the Nondimensionalized buckling load ($\bar{N}$) for a simply supported plate laminated as $[0/90]_2$ and subjected to uniform distributed load in x direction, the plot is compared with that presented by **Reddy, 2004** as a verification. It shows that $\bar{N}$ decreases very slowly with increasing aspect ratio after a/b=1.3 especially when a/b=2.3 where the difference in the load starts to be very small, and observing that the buckling occurs rapidly with increasing aspect ratio.

c- Effect of lamination angle

Assume a square plate (E_1/E_2 =40, G_{12}=0.5E_2, υ_{12}=0.25) subjected to distributed loads in x direction and has the lamination $[-\theta/\theta]_2$. From **fig. 7**, it is observed that the plot is symmetric about $\theta = 45^o$ and the buckling load is maximum for SSSS conditions (verified with **Reddy, 2004**). But for other boundary conditions, the load decreases with the increase of lamination angle.

d- Effect of Loading Type

Table (5). shows dimensionless critical buckling load ($\bar{N} = \frac{N_{cr} b^2}{E_2 h^3}$) of a simply supported and clamped plates (E_1/E_2=10, G_{12}=0.6E_2, υ_{12}=0.25, [0/90/0]) subjected to different loading types. It shows that uniformly loaded plate buckles earlier than the others, while the linearly loaded plate buckles with higher loads which means that the plate will retain more load than plate subjected to uniform load. The critical linear loads for the two boundary conditions are twice the critical uniform loads.

4.2 Investigation of Natural Frequency of Free Vibration

The natural frequency is investigated with and without the action of buckling where the critical buckling load applied to the plate is precalculated from the previous section. Several considerations are presented to investigate the natural frequency which is calculated as dimensionless form ($\bar{\omega} = \frac{\omega_o a^2}{h}\sqrt{\frac{\rho_c}{E_2}}$). In case of buckling action, a ratio (d) of critical load is applied. The effect of the load ratio (d) is studied to present the behavior of the plate and its frequency.

a- Effect of Boundary Conditions

In this analysis, a square plate (E_1/E_2=10, G_{12}=0.6E_2, υ_{12}=0.25, [0/90/0]) with various boundary conditions is taken to calculate the dimensionless natural frequency. From **Table (6**), it is found that the clamped plate vibrates with natural frequency higher than the other boundaries because of the high stiffness due to boundary. In other hand, the natural frequency for the SFSF plate is minimum due to low stiffness. The same investigation is repeated in **Table (6**) for the same plate subjected to parabolic load (load ratio d=0.5), and it is clear that the natural frequency is less than that found without loading.

b- Effect of aspect ratio

The increasing aspect ratio decreases the natural frequency, till a/b=2, where the frequency starts to converge with higher aspect ratio. **Fig. 8** shows this behavior for a $[0/90]_2$ simply supported laminate (E_1/E_2=10, G_{12}=0.6E_2, υ_{12}=0.25) with and without the action of buckling for parabolic load. It is obvious that natural frequency with buckling is lower than that without buckling.

c- Effect of lamination angle

Assume a square plate (E_1/E_2=10, G_{12}=0.6E_2, υ_{12}=0.25) but with different lamination systems and boundary conditions. From **Table (7),** it is obvious that $[45/-45]_2$ plate has the same frequency of $[45\ -45]_s$ plate, but for SFSF plate under buckling action, it is greater in symmetric than unsymmetric laminates. For the other laminates, the frequency is equal for symmetric and unsymmetric in the cases of SSSS and CCCC conditions while it is unequal for the other conditions for the same laminate. It can be seen for the two cases that the natural frequency for symmetric laminates $[0\ 90]_s$ is greater than that for unsymmetric laminates $[0/90]_2$. Oppositely; for laminates $[60\ 30]_s$, the natural frequency is less than that for unsymmetrical laminates $[60\ 30]_2$.

d- Effect of loading type and ratio

The natural frequency under buckling is almost equal for different loading types in analytical solution, where the difference is very infinitesimal, while the frequency determined by numerical solution differs with very small error, but for case of parabolic load, the discrepancy is greater than other loading cases which may reach 7% for d=0.75 of clamped plate. **Table (8)** shows the dimensionless natural frequency of a laminated plate (E_1/E_2=10, G_{12}=0.6E_2, υ_{12}=0.25, [0/90/0]) under buckling of different load functions. It is obvious that the natural frequency ($\bar{\omega} = \frac{\omega_o b^2}{\pi^2}\sqrt{\frac{\rho_c h}{D_{22}}}$) is inversely proportional to the load ratio, where the increasing in load ratio decreases the frequency.

4.3 Verification Study for Buckling and Vibration of Laminated Plate

The numerical results are obtained using programming software (ANSYS) to verify the analytic derivation. The programming in ANSYS is stepped as follows:

1- Choosing the element type (shell 281).
2- The material properties as (E_1/E_2=10, G_{12}=0.6E_2, υ_{12}=0.25).
3- The layers angles and their thicknesses ([0/90/0]).
4- Creating the model as a square plate (a/b=1).
5- Meshing the area with different sizes for convergent result.
6- Choosing the analysis type with prestress option.

7- Define the boundary conditions and loads.
8- Solving the model.
9- Reading and plotting the results.
10- Finishing the solution.

Assume two simply supported and clamped plates subjected to different loads at edges x=0, a. **Table (5)** showed the numerical and analytical dimensionless critical buckling loads ($\bar{N} = \frac{N_{cr} b^2}{E_2 h^3}$). The comparison shows a good agreement between the analytical and numerical results, where the higher discrepancy is 4% for CCCC plate under parabolic load buckling. As investigated in section 4.1, it is obvious that the buckling occurs earlier for uniform load than other loading types.

The Nondimensionalized natural frequency of the same plates found numerically for SSSS conditions to be ($\bar{\omega} = \frac{\omega_o a^2}{h}\sqrt{\frac{\rho_c}{E_2}} = 10.643$) while analytic result is ($\bar{\omega} = 10.645, discrepancy = 0.01\%$). It is clear that a high agreement between the analytical and numerical results was obtained. The numerical natural frequencies of a plate under buckling action of different loads are listed in **Table (9).** The analytical result is ($\bar{\omega} = 7.530$) for a simply supported plate subjected to the three load types. From the comparison between the results, high agreement is produced where the discrepancy does not exceed 2.8% for parabolic buckling case.

5. CONCLUSIONS

The buckling and vibration results lead to the following conclusions:

1- The number of half wavelengths affects the critical buckling load, where the increasing of aspect ratio requires larger number (half-waves number) to get more accurate results.
2- The aspect ratio affects the buckling load and natural frequency reversely. The buckling load decreases rapidly with increasing aspect ratio till it is about 1.5, after that it takes constancy or close values for higher aspect ratios. The natural frequency, decreases with high percentage until aspect ratio a/b=2, then it takes the constancy for higher ratios.
3- The boundary conditions affect the critical buckling load and fundamental natural frequency. Clamped edges conditions offer high stiffness, results in high critical buckling load and natural frequency. It is obvious for highly constrained edges, the stiffness increases which causes the plate to sustain high load and frequency. The results grade from higher to lower values as CCCC-CSCS-CFCF-SSSS and then SFSF.
4- The lamination angle has clear effect on the buckling load of the laminate, where the critical load of a simply supported plate is directly proportional to the angle under 45^o where the maximum load occurs, and then it is reversely proportional to the increasing in lamination angle. For other boundary conditions, the load is reversely proportional to the angle.
5- The plate subjected to buckling linear load can hold larger load than other loading types; the uniform load buckles the plate earlier than others. The effect of load type is very small on the natural frequency.
6- The natural frequency changes indirectly with buckling load ratio.

REFERENCES

- Amabili1, M., Karagiozis1 K., Farhadi, S., and Khorshidi K. , 2010, Nonlinear Vibration of Plates with Different Boundary Conditions using Higher Order Theory, Chaos, 3rd Chaotic Modeling and Simulation.

- Berthelot, J., 2010, Mechanics of Composite Materials and Structures, ISMANS, Institute for Advanced Le Mans, Materials and Mechanics, France.

- Brown, R. G., 2007, Introductory Physics I: Elementary Mechanics, Duke University Physics Department.

- Craciun, E.M. and Simionescu-Panait, O., 2004, Instability Critical Loads of The Fiber Reinforced Elastic Composites, Ovidius Constanta, Vol. 12(2), PP. 99-108.

- Hu, H., Badir, A., and Abatan, A., 2003, Buckling Behavior of a Graphite/Epoxy Composite Plate under Parabolic Variation of Axial Loads, International Journal of Mechanical Sciences 45, PP. 1135–1147.

- Jana, P. and Bhaskar, K., 2007, Analytical Solutions for Buckling of Rectangular Plates under Non-Uniform Biaxial Compression or Uniaxial Compression with In-Plane Lateral Restraint, International Journal of Mechanical Sciences 49, PP. 1104-1112.

- Kollar, L. A. and Springer, G. S., 2003, Mechanics of Composite Structures, Cambridge University Press.

- Kumar, M. M., Jacob, C. V., Lakshminarayana N., Puneeth, B. M., and Nagabhushana, M., 2013, *Buckling Analysis of Woven Glass Epoxy Laminated Composite Plate*, American Journal of Engineering Research (AJER), Vol. 2, Issue-7, PP. 33-40.

- Leissa, A. W. and Kang, J. , 2002, Exact Solutions for Vibration and Buckling of an SS-C-SS-C Rectangular Plate Loaded by Linearly Varying In-Plane Stresses, International Journal of Mechanical Sciences 44, PP. 1925–1945.

- Matsunaga, H., 2000, Vibration and Stability of Cross-Ply Laminated Composite Plates According to a Global Higher-Order Plate Theory, Composite Structures 48, PP. 231-244.

- Reddy, B. S., Reddy, M. R., and Reddy V. N., 2013, Vibration Analysis of Laminated Composite Plates Using Design of Experimentspproach, International Journal of Scientific Engineering and Technology, Vol. No.2, Issue No.1, PP. 40-49.

- Reddy, J.N., 2004, Mechanics of Laminated Composite Plates and Shells: Theory and Analysis, CRC Press LLC, 2nd ed..

Tang, Y. and Wang, X., 2011, *Buckling of Symmetrically Laminated Rectangular Plates under Parabolic Edge Compressions*, International Journal of Mechanical Sciences 53, PP. 91-97.

Ventsel, E. and Krauthammer, T.,2001, *Thin Plates and Shells: Theory, Analysis, and Applications*, The Pennsylvania State University, University Park, Pennsylvania.

NOMENCLATURE

A_{mn}= coefficients in the assumed series for deflection, dimensionless.
a, b= Plate length and width, m.
B_{ij}= coupling stiffness matrix elements, N.
D_{ij}= bending stiffness matrix elements, N.m.
d= Load ratio, dimensionless.
E= total mechanical energy, N.m.
Ec= total kinetic energy, N.m .
E_1,E_2= modulus of elasticity in 1 and 2 directions respectively, GPa.
G_{12}= shear modulus in plane 1-2, GPa.
h= thickness of the laminate, m.
I_o= moment of inertia of the laminate at point (*x, y*), Kg/m^2.
k= layer number.
$\kappa_x, \kappa_y, \kappa_{xy}$= curvatures of the reference plane of the plate, dimensionless.
L= total number of layers in the laminate.
M, N= upper limits of double series, dimensionless.
m, n= numbers of half wavelengths, dimensionless.
N_x= in-plane force in x direction, N/m.
$\overline{N}$= nondimensionalized buckling load, dimensionless.
N_{cr}= critical buckling load, N/m.
N_o= load intensity of distributed load, N/m.
N_o= Load intensity of distributed load, N/m.
$\overline{Q}_{ij}$= transformed reduced stiffness matrix elements, N/m.
U= strain energy of internal forces, N.m.
u, v, w= displacements in x, y, z directions, m.
u_o, v_o, w_o= displacement components along the (*x, y, z*) coordinate directions, m.
v_f= fiber Volume fraction, dimensionless.
$X_m(x)$, $Y_n(y)$= functional bases for boundary conditions, dimensionless.
zk and *zk-1*= distances from the reference plane of the laminate to the two surfaces of the *kth* ply, m.
γ, λ= constants of boundary conditions functions, dimensionless.
δ= variation of a amount, dimensionless.
θ= Angle of layer lamination, Degree.
υ_{12}= poisson ratio in plane 1-2, dimensionless.
Π= total potential energy, N.m.
ρ= density of material, Kg/m^3.
ρ_c, ρ_f, ρ_m= densities of the composite, fiber, and matrix respectively, Kg/m^3.
Ω= work of external forces, N.m.

ω= natural frequency of the plate vibrations, Hz.
$\bar{\omega}$= nondimensionalized natural frequency, dimensionless.

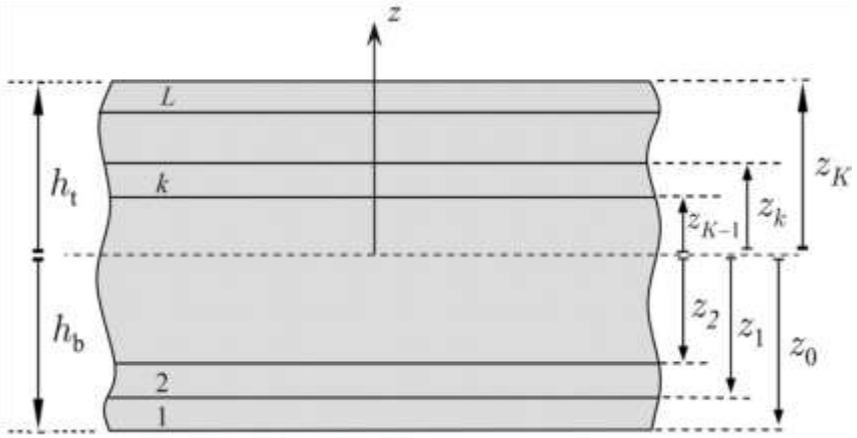

Figure 1. Distances from the reference plane.

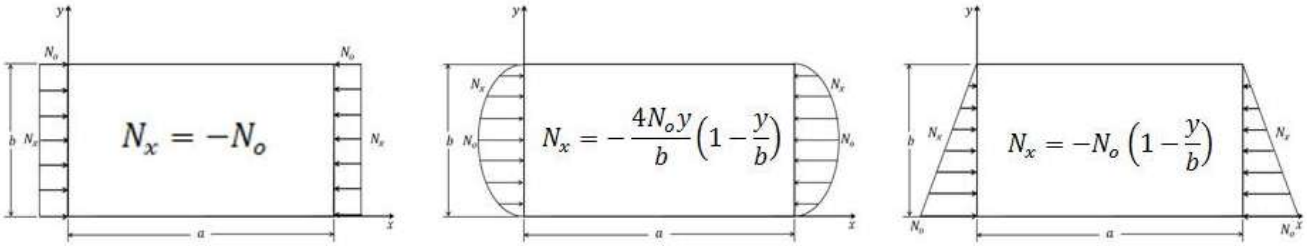

Figure 2. Plates subjected to distributed loads.

Figure 3. Specimen molding process

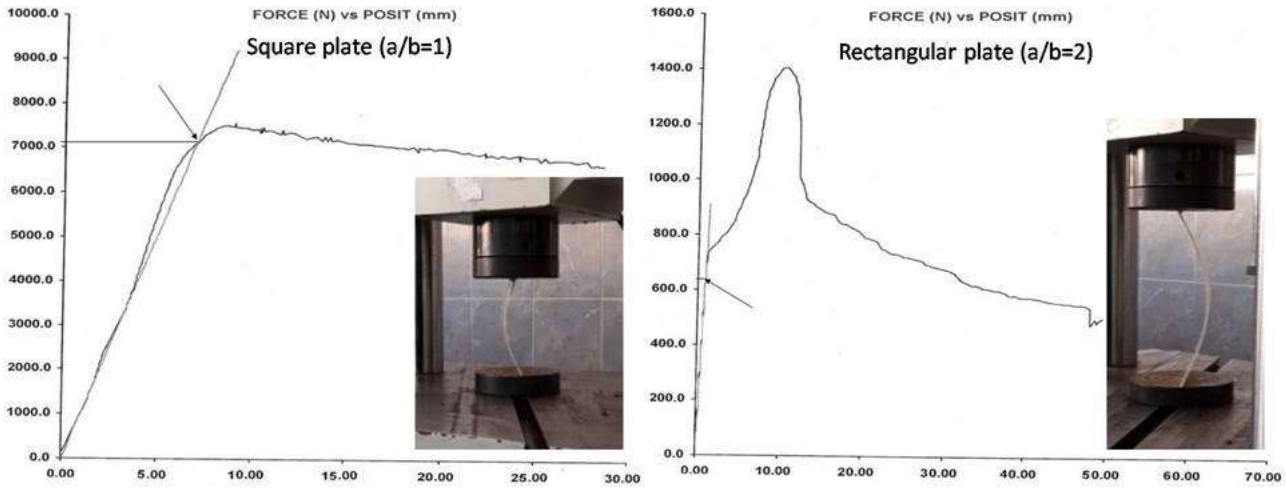

Figure 4. Load displacement curves of the Buckled plates.

(a) **(b)**

Figure 5. a) Free vibration test setup; (1) Power supply, (2) Impact hammar, (3) Testing structure, (4) weights, (5) Tested plate, (6) Accelerometer, (7) Charge amplifier for Accelerometer, (8) Oscilloscope; **b)** Generated response and FFT wave.

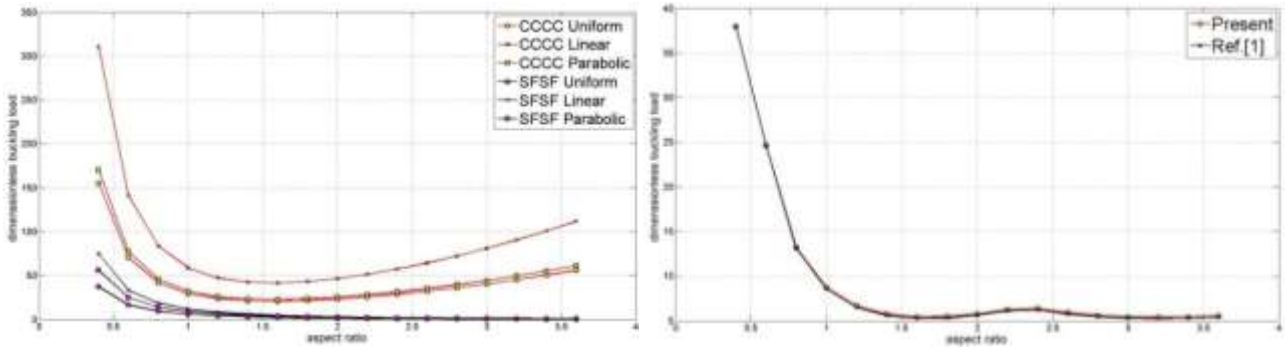

(**a**) **(b)**

Figure 6. Nondimensionalized buckling load ($\bar{N}$) versus aspect ratio for: **a)** CCCC and SFSF; **b)** SSSS orthotropic plates $[0/90]_2$.

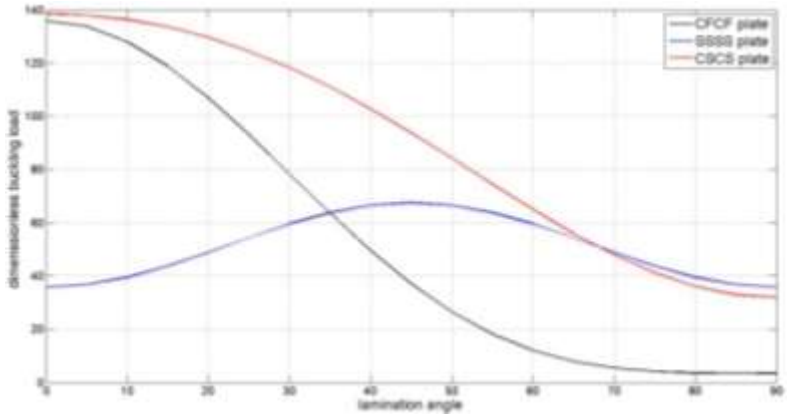

Figure 7. Nondimensionalized buckling load ($\bar{N} = \frac{N_{cr}b^2}{E_2h^3}$) versus lamination angle (θ) of antisymmetric angle-ply square laminates under uniaxial uniform compression.

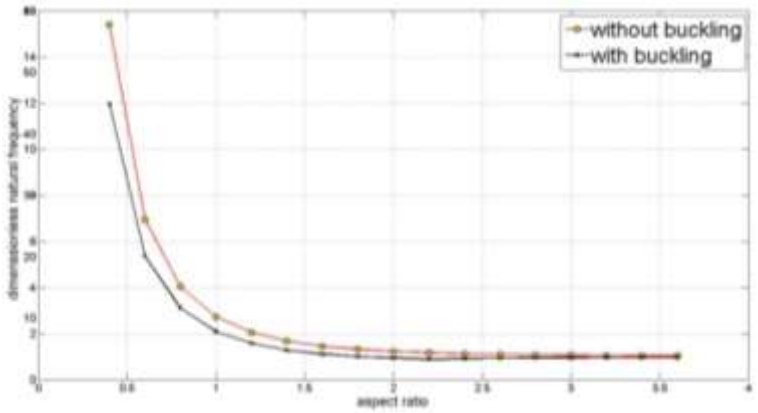

Figure 8. Nondimensionalized fundamental frequency ($\bar{\omega} = \frac{\omega_o b^2}{\pi^2}\sqrt{\frac{\rho_c h}{D_{22}}}$) versus aspect ratio of SSSS symmetric laminates subjected to parabolic load.

Table 1. Values of the constants λ_i and γ_i of the plate functions in the case of clamped and free ends of the plate.

m=n=i	λ_i		γ_i	
	Clamped	Free	Clamped	Free
1	4.7300	0	0.9825	
2	7.8532	0	1.0007	
3	10.9956	4.730	0.9999	–0.9825
4	14.1371	7.853	1.0000	–1.0008
5	17.2787	10.996	0.9999	–1.000
6	20.4203	14.137	1.0000	–1.000
7	23.5619	17.279	1.0000	–1.000
8	26.7035	20.420	1.0000	–1.000

Table 2. Experimental mechanical properties of E-glass/Polyester composite plate.

Physical and Mechanical Property	Obtained Result
$\rho_f(Kg/m^3)$	2360
$\rho_m(Kg/m^3)$	970
$\rho_c(Kg/m^3)$	1369
E_1(GPa)	26.285
E_2(GPa)	5.882
G_{12}(GPa)	2.213
ν_{12}	0.25
V_f	0.323

Table 3. Experimental non-dimensional critical buckling loads $\frac{N_{cr}b^2}{E_2h^3}$ of the tested plates.

Plate Geometry (cm)	20×20×0.25	40×20×0.2
Aspect Ratio a/b	1	2
Angle Ply Orientations	$[0/90]_s$	$[0/90]_2$
Experimental Result	3.097	0.538
Analytical Result	3.398	0.575
Discrepancy%	8.8	6.4

Table 4. Nondimensionalized buckling load ($\bar{N}$) of a square plate laminated as (0/90/0) and subjected to uniaxial edge loads (The results between the brackets represent the numerical results for comparison. The subscript refers to (m=n)).

Type of applied load	**Type of boundary conditions**				
	$SSSS_1$	$CCCC_1$	$CSCS_1$	$SFSF_3$	$CFCF_1$
Uniform load	11.491 (11.559)	40.507 (40.777)	36.255 (36.276)	7.991 (8.018)	32.982 (32.968)
Parabolic load	13.219 (13.694)	44.395 (46.207)	41.705 (42.83)	11.279 (11.638)	49.473 (46.462)
Linear load	22.983 (22.838)	81.015 (80.11)	72.510 (70.481)	11.120 (11.327)	65.964 (64.391)

Table 5. Nondimensionalized buckling load ($\bar{N}$) of a SSSS and CCCC square plate laminated as (0/90/0) and subjected to uniaxial edge loads.

Type of Load	**Boundary Conditions**					
	SSSS			**CCCC**		
	Analytical Result	Numerical Result	discrepancy	Analytical Result	Numerical Result	discrepancy
Uniform	11.491	11.6	0.9%	40.507	40.8	0.7%
Parabolic	13.219	13.7	3.6%	44.395	46.2	4%
Linear	22.983	22.8	0.7%	81.015	80.1	1.1%

Table 6. Nondimensionalized fundamental frequency of a symmetric cross-ply square plate of various boundary conditions (the results between the brackets refer to the Nondimensionalized fundamental frequency of the same plate subjected to parabolic load of load ratio d=0.5).

Boundary Conditions	**Analytical results**	**Numerical results**	**Discrepancy%**	**Other Researches**
SSSS	10.649 (7.530)	10.645 (7.613)	0.03 (1.1)	10.650[Reference 1]
CCCC	22.323 (15.785)	22.310 (16.237)	0.05 (2.8)	————
CSCS	21.119 (14.933)	21.115 (15.256)	0.01 (2.1)	21.118[Reference 1]
SFSF	8.886 (5.973)	8.875 (5.774)	0.1 (3.3)	————

Table 7. Nondimensionalized fundamental frequency ($\frac{\omega_o b^2}{\pi^2}\sqrt{\frac{\rho h}{D_{22}}}$) of a square plate of various laminations and boundary conditions (d=0.5 for buckled plate).

Angle Ply		**Type of boundary conditions**				
		SSSS	CCCC	CSCS	SFSF	CFCF
$[0\ 90]_s$	Without Buckling	2.556 (2.555)	5.358 (5.312)	4.914 (4.913)	1.988 (2.041)	4.632 (4.630)
	With Buckling	1.807 (1.755)	3.788 (3.603)	3.475 (3.569)	1.688 (1.631)	3.275 (3.095)
[0 90 0 90]	Without Buckling	1.588 (1.601)	3.330 (3.398)	2.606 (2.586)	0.956 (1.002)	2.266 (2.317)
	With Buckling	1.123 (1.146)	2.355 (2.237)	1.842 (1.766)	0.801 (0.950)	1.602 (1.577)
$[60\ 30]_s$	Without Buckling	1.877 (1.815)	3.242 (3.101)	2.391 (2.287)	0.781 (0.711)	1.441 (1.491)
	With Buckling	1.327 (1.397)	2.292 (2.131)	1.691 (1733)	0.846 (0.873)	1.019 (0.971)
[60 30 60 30]	Without Buckling	2.240 (2.318)	3.869 (3.633)	3.146 (3.358)	0.869 (0.912)	2.266 (2.199)
	With Buckling	1.584 (1.501)	2.735 (2.613)	2.225 (2.399)	1.010 (1.138)	1.602 (1.423)
$[45\ -45]_s$	Without Buckling	2.517 (2.728)	4.125 (4.492)	3.397 (3.152)	1.070 (0.910)	2.267 (1.986)
	With Buckling	1.780 (1.694)	2.916 (3.089)	2.402 (2.495)	1.187 (1.036)	1.602 (1.554)
[45 -45 45 -45]	Without Buckling	2.517 (2.311)	4.125 (4.016)	3.397 (3.248)	0.486 0.441)	2.267 (2.252)
	With Buckling	1.780 (1.701)	2.916 (3.052)	2.402 (2.258)	0.711 (0.730)	1.602 (1.523)

Table 8. Dimensionless natural frequency of a laminated plate under buckling of different load functions and ratios (superscripts refer to the first letter of the load type).

d	Type of boundary condition				
	SSSS	CCCC	CSCS	SFSF	CFCF
0	10.649 (10.645)	22.323 (22.310)	21.119 (21.115)	8.886 (8.875)	20.143 (20.133)
0.25	9.223 $(9.231)^{U}$ $(9.275)^{P}$ $(9.218)^{L}$	19.332 $(19.353)^{U}$ $(19.530)^{P}$ $(19.305)^{L}$	18.290 $(18.352)^{U}$ $(18.451)^{P}$ $(18.259)^{L}$	7.443 $(7.403)^{U}$ $(7.322)^{P}$ $(7.501)^{L}$	17.444 $(17.121)^{U}$ $(17.988)^{P}$ $(17.673)^{L}$
0.5	7.530 $(7.544)^{U}$ $(7.613)^{P}$ $(7.522)^{L}$	15.785 $(15.785)^{U}$ $(16.219)^{P}$ $(15.638)^{L}$	14.933 $(15.040)^{U}$ $(15.256)^{P}$ $(14.947)^{L}$	5.973 $(5.877)^{U}$ $(6.212)^{P}$ $(5.834)^{L}$	14.243 $(14.405)^{U}$ $(13.899)^{P}$ $(14.011)^{L}$
0.75	5.324 $(5.379)^{U}$ $(5.583)^{P}$ $(5.378)^{L}$	11.161 $(11.013)^{U}$ $(11.948)^{P}$ $(11.282)^{L}$	10.559 $(10.66)^{U}$ $(11.115)^{P}$ $(10.685)^{L}$	3.995 $(3.910)^{U}$ $(4.197)^{P}$ $(3.980)^{L}$	10.071 $(9.901)^{U}$ $(10.100)^{P}$ $(10.227)^{L}$

Table 9. Nondimensionalized natural frequency ($\bar{\omega}$) of a SSSS and CCCC square plate laminated as (0/90/0) and subjected to uniaxial edge loads.

Type of Load	SSSS	Discrepancy	CCCC	Discrepancy
No Load	10.643	0.01%	22.310	0.05%
Uniform Load	7.546	0.2%	15.839	0.3%
Parabolic load	7.621	1.2%	16.235	2.8%